

Figure 2 shows the calculated result for the quasisteady regime $\bar{T}_w = 150^\circ\text{C}$ with $\bar{\tau}^e = 1080$ sec, $\bar{\lambda}^e = 4.921$ W/m·deg, and $c_p = 10^3$ J/kg·deg. The value of thermal conductivity $\bar{\lambda}^e$ was determined by interpolation from Table 1.

Values of effective thermal conductivity in Table 2 were used to calculate the temperature relation $T(\tau)$ at the point $b = 0.026$ m for nonsteady regimes (Fig. 3). In determining $\bar{\lambda}_i^e$, we broke each of the nonsteady regimes $\bar{T}_w(\tau)$ down into three sections with respect to time. In each section, heating was assumed to be quasisteady. Accordingly, each section in Table 1 was calculated by interpolation of the thermal conductivities.

Comparison of the results calculated by simplified model (1)-(3) and data from a numerical experiment on a multilayered cylindrical shell showed that the error of the relation found here $T(\tau)$ is within the permissible range.

NOTATION

τ^e , Duration of regime; λ^e , effective thermal conductivity; $T(x, t)$, temperature; x , running coordinate; τ , running time; c , specific heat; ρ , density; d , thickness of plate; q , heat flux; T_w , temperature of heated wall.

LITERATURE CITED

1. A. T. Usov, Approximate Methods of Calculating Temperatures of Unsteadily Heated Solids of Simple Shape [in Russian], Mashinostroenie, Moscow (1973).
2. P. G. Krukovskii, "Numerical solution of inverse heat-conduction problems for multilayered structures," in: Inverse Problems and Identification of Heat-Transfer Processes: Summary of Documents of the Fifth All-Union Seminar, UAI, Ufa (1984), p. 180.
3. R. P. Fedorenko, Approximate Solution of Optimum Control Problems [in Russian], Nauka, Moscow (1978).
4. O. M. Alifanov, Identification of Heat-Transfer Processes in Aircraft [in Russian], Mashinostroenie, Moscow (1979).
5. A. A. Goryachev and V. M. Yudin, "Solution of an inverse coefficient problem of heat conduction," Inzh.-Fiz. Zh., 43, No. 4, 641-648 (1982).

GRID METHOD FOR CALCULATION OF FLOW AND HEAT EXCHANGE OF A VISCOUS INCOMPRESSIBLE LIQUID

N. I. Nikitenko

UDC 532.516:536.25

An explicit difference method is described for calculation of the flow and heat exchange of an incompressible liquid, allowing calculations at quite large Reynolds numbers.

The development of simple and effective numerical methods for modeling liquid flow and heat exchange processes at high Reynolds and Grashof numbers is of great importance in many fields of contemporary technology. Use of the algorithm presented in [1] by the present author, involving a scaled explicit difference scheme, permits successful solution of the boundary-layer problem and natural convection of a gas [2].

The present study will offer a numerical method based on the scaled difference scheme for calculating flow and heat exchange of a viscous incompressible liquid over a wide range of Grashof and Reynolds numbers.

Technical Thermophysics Institute, Academy of Sciences of the Ukrainian SSR, Kiev.
Translated from Inzhenerno-Fizicheskii Zhurnal, Vol. 50, No. 3, pp. 476-482, March, 1986.
Original article submitted December 3, 1984.

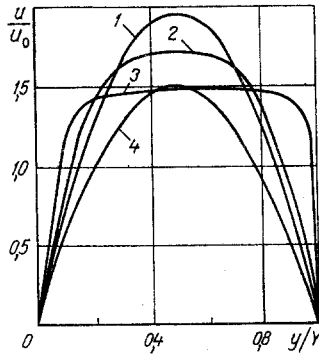


Fig. 1

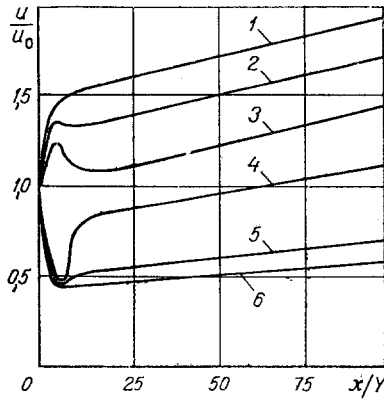


Fig. 2

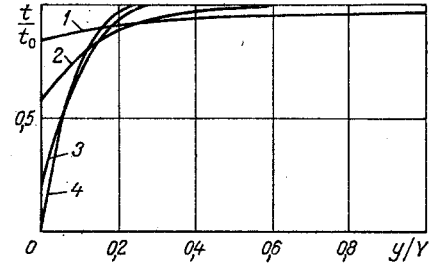


Fig. 3

Fig. 1. Relative longitudinal velocity profile u/u_0 in channel section $X/Y = 100$ for various Reynolds numbers and relative transverse velocities $\bar{v}' = v'/u_0$ of liquid transport through permeable wall: 1) $Re = 10^2$, $\bar{v}' = 0.03$; 2) 10^3 and 0.03 ; 3) 10^6 and 0.003 ; 4) 10^2 and 0 .

Fig. 2. Change in relative longitudinal velocity over channel length for various Re and relative distances $\bar{y} = y/Y$ from permeable wall: 1) $Re = 10^2$, $\bar{y} = 0.5$; 2) 10^3 and 0.5 ; 3) 10^6 and 0.5 ; 4) 10^6 and 0.083 ; 5) 10^3 and 0.083 ; 6) 10^2 and 0.083 .

Fig. 3. Relative temperature profiles t/t_0 in channel section $x/Y = 100$ for various Reynolds numbers: 1) $Re = 10^2$; 2) 10^3 ; 3) 10^4 ; 4) 10^6 .

In many cases of flow and heat exchange study liquids can be considered incompressible. For the basic dependent variables in calculations of such processes one usually uses the flow function ψ , the vorticity ω , and the temperature t . The components of the velocity vector are then determined by differentiating the flow function with respect to the coordinates, while the pressure can be found after calculating the functions ψ , ω , t by solving the corresponding Poisson-type equation [3]. We will write the flow and heat exchange equations in divergent form in the variables ω , ψ , t

$$\frac{\partial \omega}{\partial \tau} + \frac{\partial u \omega}{\partial x} + \frac{\partial v \omega}{\partial y} = v \left(\frac{\partial^2 \omega}{\partial x^2} + \frac{\partial^2 \omega}{\partial y^2} \right) - \beta \left(g_y \frac{\partial t}{\partial x} - g_x \frac{\partial t}{\partial y} \right), \quad (1)$$

$$\frac{\partial^2 \psi}{\partial x^2} + \frac{\partial^2 \psi}{\partial y^2} - \omega = 0, \quad (2)$$

$$\frac{\partial t}{\partial \tau} + \frac{\partial ut}{\partial x} + \frac{\partial vt}{\partial y} = a \left(\frac{\partial^2 t}{\partial x^2} + \frac{\partial^2 t}{\partial y^2} \right), \quad (3)$$

$$u = \frac{\partial \psi}{\partial x}, \quad v = -\frac{\partial \psi}{\partial y}, \quad \omega = \frac{\partial u}{\partial y} - \frac{\partial v}{\partial x}. \quad (4)$$

To realize system (1)-(4) numerically we approximate the vorticity transfer Eq. (1) and energy Eq. (3) with the scaled difference method of [1], which is within the class the additive methods having net approximation [4]. In accordance with this technique the differential transfer equation is correlated to two difference equations, and the desired function is calculated at each time step in two approximations. The difference equation for the first approximation approximates an incomplete transfer equation, in which only convective terms and the time derivative are retained. The difference equation for determining the unknown function in the second approximation is constructed by approximating all terms of the original differential transfer equation. On the grid

$$\begin{aligned} x_{i+1} &= x_i + h_i, \quad i = 0, 1, \dots, I; \quad y_{m+1} = y_m + h_{ym}, \\ m &= 0, 1, \dots, M; \quad \tau_{n+1} = \tau_n + l_n, \quad n = 0, 1, \dots, \end{aligned} \quad (5)$$

the difference equations which serve to determine approximate values φ_{im}^n of the functions $\varphi(\tau_n, x_i, y_m)$, $\varphi = \omega, t$, and approximate Eqs. (1), (3) with an error $O(l_n + h_i^2 + h_{ym}^2)$ have the form

$$\delta_{\tau}\bar{\omega} + \delta_x(u\bar{\omega}) + \delta_y(v\bar{\omega}) = 0, \quad (6)$$

$$\delta_{\tau}\omega + \delta_x(u\bar{\omega}) + \delta_y(v\bar{\omega}) = \nu(\delta_{xx}\bar{\omega} + \delta_{yy}\bar{\omega}) - \beta(g_y\delta_x t - g_x\delta_y t), \quad (7)$$

$$\delta_{\tau}\bar{t} + \delta_x(u\bar{t}) + \delta_y(v\bar{t}) = 0, \quad (8)$$

$$\delta_{\tau}t + \delta_x(u\bar{t}) + \delta_y(v\bar{t}) = a(\delta_{xx}\bar{t} + \delta_{yy}\bar{t}). \quad (9)$$

Here

$$\begin{aligned} \delta_{\tau}\varphi &= \delta_{\tau}\varphi_{im}^n = \frac{1}{l_n}(\varphi_{im}^{n+1} - \varphi_{im}^n), & \delta_{\tau}\bar{\varphi} &= \frac{1}{l_n}(\bar{\varphi}_{im}^{n+1} - \varphi_{im}^n), \\ \delta_x\varphi &= \frac{1}{h_i + h_{i+1}} \left[(\varphi_{i+1,m}^n - \varphi_{im}^n) \frac{h_i}{h_{i+1}} + (\varphi_{im}^n - \varphi_{i-1,m}^n) \frac{h_{i+1}}{h_i} \right], \\ \delta_{xx}\varphi &= \frac{2}{h_i + h_{i+1}} \left[(\varphi_{i+1,m}^n - \varphi_{im}^n) \frac{1}{h_{i+1}} - (\varphi_{im}^n - \varphi_{i-1,m}^n) \frac{1}{h_i} \right], \\ \varphi &= \omega, \bar{\omega}, t, \bar{t}, u\omega, u\bar{\omega}, v\omega, v\bar{\omega}, ut, u\bar{t}, vt, v\bar{t}. \end{aligned}$$

The derivatives along the y-coordinate and approximated in the same was as those along x.

The necessary conditions for stability of the solution of difference Eqs. (6)-(9), which can be found by conditional specification of some unknown system functions [1, 2], appear as follows:

$$l_n \leq \min \left\{ \left(\frac{u_{im}^n}{h_i} + \frac{v_{im}^n}{h_{ym}} \right)^{-1}, \left[4\chi^2 \left(\frac{1}{h_i^2} + \frac{1}{h_{ym}^2} \right) \right]^{-1} \right\}, \quad \chi = \nu, a. \quad (10)$$

The equation for the flow function, Eq. (2), which is elliptical, is solved at each time step by the establishment method using a three-layer explicit difference scheme [5]. On a grid which differs from Eq. (5) in that the real time τ_n is replaced by the discrete variable $\tau_k = k\tau_{\psi}$, $k = 0, 1, \dots$, $\tau_{\psi} = \text{const}$, the difference equation which will find Eq. (2) in the layer $k + 1$ has the form

$$(1 + \gamma)\delta_{\tau}\psi_{im}^k - \gamma\delta_{\tau}\psi_{im}^{k-1} = \delta_{xx}\psi_{im}^k + \delta_{yy}\psi_{im}^k - \omega_{im}^{n+1}, \quad (11)$$

where γ is a positive constant: $\delta_{\tau}\psi^k = (\psi_{im}^{k+1} - \psi_{im}^k)/\tau_{\psi}$. Although this is a three-layer scheme its computer realization requires only two data blocks R and R_1 , containing $(I + 1)(M + 1)$ elements each. At the beginning of the cycle for calculating the function ψ_{im}^{k+1} the data block R holds the function ψ_{im}^{k-1} , while R_1 holds ψ_{im}^k . The values of ψ_{im}^{k+1} for the $k + 1$ step are stored in R. After calculations for the step $k + 1$ are performed data are transferred from R to R_1 and from R_1 to R.

The condition for stability of difference Eq. (11), which can be obtained by the Fourier integral method, imposes the following limitation on the ratio between the steps of the difference grid:

$$l_{\psi} \leq \frac{1 + 2\gamma}{2(h_i^{-2} + h_{ym}^{-2})}. \quad (12)$$

By varying the parameter γ any desired grid steps can be selected. However, results of numerical experiments show that minimum machine time expenditure for establishing the solution to the flow function equation is achieved at a value $\gamma = 2-2.5$, which corresponds to a 5-6-fold increase in the time step as compared to the maximum for a conventional two-layer explicit difference scheme. We note that the step τ_{ψ} is in fact an iteration parameter in the search for ψ_{im}^{n+1} . The process of establishing the solution to Eq. (11) is considered completed when the condition $\sum_i \sum_m |\delta_{\tau}\psi_{im}^k| < \Delta$ is satisfied, where Δ is a small positive number. It is assumed here that $\psi^{n+1} = \psi^k$. For the initial approximation corresponding to the value $k = 0$, we take $\psi^k = \psi^n$. The components of the velocity vector u_{im}^{n+1} and v_{im}^{n+1} are determined from difference equations stemming from Eq. (4)

$$u_{im}^{n+1} = \delta_y\psi_{im}^{n+1}; \quad v_{im}^{n+1} = -\delta_x\psi_{im}^{n+1}.$$

It should be noted that the replacement in Eq. (7) of the term $\delta_\tau \omega$ by the operator $(1 + \gamma_\omega) \delta_\tau \omega_{im}^n - \gamma_\omega \delta_\tau \omega_{im}^{n-1}$ ($\gamma_\omega > 0$) or the value ω_{im}^{n+1} by $\bar{\omega}_{im}^{n+1}$ in the approximations $\delta_{xx} \bar{\omega}$ and $\delta_{yy} \bar{\omega}$ allows a significant easing of the limitation on the time step τ_n for relatively small spatial steps.

We will now consider a calculation with the method described above of forced flow and heat exchange in the initial section of a channel $0 < x < X$, one wall of which is permeable. The initial velocity and temperature distributions are taken homogeneous:

$$u(0, x, y) = v(0, x, y) = 0, t(0, x, y) = t_i \quad (13)$$

In the initial channel section $x = 0$

$$u(\tau, 0, y) = u_0(\tau, y), v(\tau, 0, y) = 0, t(\tau, 0, y) = t_0(\tau, y). \quad (14)$$

On the right-hand permeable channel boundary $y = 0$ the following conditions are satisfied:

$$\begin{aligned} u(\tau, x, 0) = 0, v(\tau, x, 0) = v', \\ \lambda \frac{\partial t(\tau, x, 0)}{\partial y} = (\alpha' - \varepsilon v' c \rho) [t(\tau, x, 0) - t'_c], \\ \varepsilon = 0 \text{ for } v' \leq 0, \varepsilon = 1 \text{ for } v' > 0. \end{aligned} \quad (15)$$

On the left-hand channel boundary

$$u(\tau, x, Y) = v(\tau, x, Y) = 0, \lambda \frac{\partial t(\tau, x, Y)}{\partial y} = -\alpha'' [t(\tau, x, Y) - t''_m]. \quad (16)$$

The conditions at the output boundary $x = X$ will be written with the assumption that near this boundary the flow is stabilized and its characteristics change quite slowly along the flow lines, i.e.,

$$\frac{\partial^s \varphi}{\partial x^s} \approx 0, \varphi = u, v, t, \omega; s = 1, 2, \dots \quad (17)$$

Aside from the basic uniqueness conditions presented above, for numerical realization of the mathematical model we use additional mass balance conditions

$$\int_0^Y u(\tau, 0, y) dy + \int_0^X v(\tau, x, 0) dx + \int_0^X v(\tau, x, Y) dx + \int_0^Y u(\tau, X, y) dy = 0. \quad (18)$$

The first, second, third, and fourth terms on the left of Eq. (10) are the liquid flow rates through the boundaries $x = 0$, $y = 0$, $y = Y$, and $x = X$, respectively.

The numerical solution of this problem is carried out in the following sequence. In the layer $n = 0$, corresponding to the initial moment $\tau = 0$, the values of the unknown grid functions u, v, ω, ψ, t are defined by conditions (13) and Eq. (4):

$$u_{im}^0 = v_{im}^0 = \omega_{im}^0 = \psi_{im}^0 = 0, t_{im}^0 = t_i \quad (19)$$

We assume that the values of these functions for time layers 1, 2, ..., n have already been found, and that values must be determined for layer n + 1. Initially, using Eqs. (6), (8), we calculate preliminary values of the functions $\bar{\omega}_{im}^{n+1}$ and \bar{t}_{im}^{n+1} at the internal grid points $i = 1, 2, \dots, I - 1$; $m = 1, 2, \dots, M - 1$. At the limiting grid points we take

$$\bar{\omega}_{im}^{n+1}|_b = \omega_{im}^n|_b, \bar{t}_{im}^{n+1}|_b = t_{im}^n|_b. \quad (20)$$

Then we use Eqs. (7), (9) to calculate the final values of the functions ω_{im}^{n+1} and t_{im}^{n+1} in the n + 1 layer at internal grid points. The values of the functions t_{im}^{n+1} at the limiting grid points are determined from the conditions:

$$t_{0m}^{n+1} = t_0(\tau_{n+1}, y_m), t_{im}^{n+1} = 2t_{i-1,m}^{n+1} - t_{i-2,m}^{n+1}, m = 1, 2, \dots, M - 1, \quad (21)$$

$$\frac{\lambda}{h_0} (t_{i,1}^{n+1} - t_{i,0}^{n+1}) = (\alpha' - \varepsilon (v')^n c \rho) (t_{i0}^{n+1} - t'_c), i = 1, 2, \dots, I - 1, \quad (22)$$

$$\frac{\lambda}{h_{y,M-1}} (t_{i,M}^{n+1} - t_{i,M-1}^{n+1}) = -\alpha'' (t_{iM}^{n+1} - t''_c), i = 1, 2, \dots, I - 1. \quad (23)$$

The grid function ψ_{im}^{n+1} is then calculated immediately. At the input section and on the side walls of the channel to find ψ_{im}^{n+1} in terms of the velocity functions specified on these boundaries we use difference equations stemming from Eq. (4):

$$\begin{aligned}\psi_{0,m+1}^{n+1} &= \psi_{0m}^{n+1} + \frac{h_{ym}}{2} (u_{0,m+1}^{n+1} + u_{0m}^{n+1}), \\ \psi_{i+1,0}^{n+1} &= \psi_{i0}^{n+1} - \frac{h_i}{2} (v_{i+1,0}^{n+1} + v_{i,0}^{n+1}), \\ \psi_{i+1,M}^{n+1} &= \psi_{iM}^{n+1} - \frac{h_i}{2} (v_{i+1,M}^{n+1} + v_{i,M}^{n+1}).\end{aligned}\tag{24}$$

With respect to simplicity, accuracy, and stability of the solution the following method of finding the function ψ_{im}^{n+1} at the output boundary of the flow can be recommended. In accordance with Eq. (17) on the boundary $x = X$ we find the longitudinal velocity \bar{u}_{im}^{n+1} in the first approximation

$$\bar{u}_{im}^{n+1} = 2u_{i-1,m}^n - u_{i-2,m}^n.\tag{25}$$

The second approximation is obtained with the relationship

$$u_{im}^{n+1} = \beta^{n+1} \bar{u}_{im}^{n+1},\tag{26}$$

where the coefficient β^{n+1} is determined from mass balance Eq. (18). The first, second, and third terms on the left side of Eq. (18) can be expressed, for example, in terms of the normal components of the velocity vector on the boundaries $x = 0$, $y = 0$, and $y = Y$, using the trapezoid expression, while the fourth term is expressed in terms of the velocity u_{im}^{n+1} . The difference analog to the balance equation obtained in this manner is solved for the first unknown function β^{n+1} . The values of ψ_{im}^{n+1} are found in terms of u_{im}^{n+1} with relationships analogous to Eq. (24).

The boundary values of the flow function on the layer $n + 1$ are used to determine ψ_{im}^{n+1} with Eq. (11) at internal grid points, after which u_{im}^{n+1} and v_{im}^{n+1} are determined with Eq. (14).

Determination of the unknown function on the layer $n + 1$ is completed by calculating the vorticity ω at the boundary grid points with expressions obtained assuming the smoothness of the functions ω :

$$\begin{aligned}\omega_{0m}^{n+1} &= \delta_y u_{0m}^{n+1} + \frac{2}{h_0^2} (\psi_{1m}^{n+1} - \psi_{0m}^{n+1} + v_{0m}^{n+1} h_0), \\ \omega_{im}^{n+1} &= \delta_y u_{im}^{n+1} + \frac{2}{h_{i-1}^2} (\psi_{i-1,m}^{n+1} - \psi_{im}^{n+1} - v_{im}^{n+1} h_{i-1}), \\ \omega_{i0}^{n+1} &= -\delta_x v_{i0}^{n+1} + \frac{2}{h_{y0}^2} (\psi_{i1}^{n+1} - \psi_{i0}^{n+1} - u_{i0}^{n+1} h_{y0}), \\ \omega_{iM}^{n+1} &= 2\omega_{i,M-1}^{n+1} - \omega_{i,M-2}^{n+1}.\end{aligned}\tag{27}$$

For natural convection problems the algorithm simplifies somewhat, since in this case for the boundary grid points $v = u = \psi = 0$. The computation time τ_s on a BESM-4M computer for one time step is approximately $\tau_s \approx 0.005D$, where D is the number of nodes in the grid.

Figures 1-3 show some results of velocity and temperature field calculations in a slot channel at various Reynolds numbers $Re = u_0 Y / \nu$ on the basis of Eqs. (6)-(27).

The relative liquid velocity through the permeable wall $v'/u_0 = 0.003$; the Prandtl number $Pr = a/\nu = 1$; mass forces are absent, i.e., $g_x = g_y = 0$; the velocity u_0 and temperature t_0 in the input section are constant. The relative channel length X/Y was varied from 1 to 200. According to Fig. 1, an increase in Re causes the velocity profile to become more filled. At larger Re this profile takes on the form characteristic of a turbulent flow regime in channels with both permeable and impermeable walls. It is evident from Fig. 2 that with increase in Reynolds number nonuniformity in the change in velocity profile over channel length near the input section increases. As follows from Fig. 3, for identical liquid velocities v'/u_0

through the permeable wall the temperature of the latter decreases with increase in Re , and at sufficiently high Re the temperature of the wall and the liquid traveling toward it coincide.

The results of the numerical experiments indicate the effectiveness of the difference method described over a wide range of Reynolds and Grashof numbers.

NOTATION

x, y , Spatial coordinates; τ , time; u, v , projections of velocity vector on x and y axes; ψ , flow function; ω , vorticity; t , temperature; g_x, g_y , projections of acceleration created by external mass forces along x and y axes; β , temperature expansion coefficient; $\nu, \lambda, \alpha, \alpha$, coefficients of kinematic viscosity, thermal conductivity, heat liberation, and thermal diffusivity; ρ, c , density and specific heat of liquid; t_m , temperature of external medium surrounding channel wall.

LITERATURE CITED

1. N. I. Nikitenko, Study of Nonsteady-State Heat and Mass Exchange Processes by the Grid Method [in Russian], Naukova Dumka, Kiev (1971).
2. N. I. Nikitenko, Theory of Heat and Mass Exchange [in Russian], Naukova Dumka, Kiev (1983).
3. P. J. Roache, Computational Fluid Dynamics, Hermosa (1976).
4. A. A. Samarskii, Theory of Difference Methods [in Russian], Nauka, Moscow (1977).
5. N. I. Nikitenko and Yu. N. Nikitenko, "Study of heat-mass exchange in crystallization of alloys with consideration of the two-phase zone," *Promyshl. Teplotekh.*, 5, No. 6, 7-13 (1983).

A NUMERICAL METHOD OF CALCULATING THE BOUNDARY OF STABILITY OF THERMALLY INDUCED ACOUSTIC OSCILLATIONS

V. A. Sysoev, S. P. Gorbachev,
and V. K. Matyushchenkov

UDC 621.59:534.1:546.291

We present the results of a theoretical and experimental study of the conditions under which thermally induced acoustic oscillations arise in nonisothermal pipelines of variable cross section.

In cryogenic nonisothermal pipelines, closed at the warm end and open at the cold end, thermally induced oscillations can arise, accompanied by a large heat flux in the low temperature zone. The stability boundary of such oscillations determines the conditions under which they arise and it depends on the wall temperature profiles of the pipeline and its cross section. For the case in which the temperature distribution and the pipeline cross section along its length are specified by single-step functions, a stability analysis was given in [1-4]. In [5] a numerical study was made of the influence of the temperature profile on the stability of the oscillations. In the present paper we solve the very same problem, but for a pipeline of variable cross section.

The set of equations with respect to the amplitude for the oscillations of a gas with a frequency ω in a nonisothermal tube of variable cross section has the form [4].

$$i\omega\rho + \frac{\rho_0}{r_0^2(x)} \frac{\partial}{\partial x} (r_0^2(x) U) + \frac{\partial\rho_0}{\partial x} U = 0, \quad (1)$$

Balashov Scientific-Industrial Organization of Cryogenic Machine Construction. Translated from *Inzhenerno-Fizicheskii Zhurnal*, Vol. 50, No. 3, pp. 483-487, March, 1986. Original article submitted December 14, 1984.